NATIONAL ADVISORY COMMITTEE FOR AERONAUTICS

TECHNICAL NOTE 3314

A TECHNIQUE UTILIZING ROCKET-PROPELLED TEST VEHICLES FOR THE MEASUREMENT OF THE DAMPING IN ROLL OF STING-MOUNTED MODELS AND SOME INITIAL RESULTS FOR DELTA AND UNSWEPT TAPERED WINGS

By William M. Bland, Jr., and Carl A. Sandahl

Langley Aeronautical Laboratory
Langley Field, Va.

Washington
May 1955

NATIONAL ADVISORY COMMITTEE FOR AERONAUTICS

TECHNICAL NOTE 3314

A TECHNIQUE UTILIZING ROCKET-PROPELLED TEST VEHICLES FOR THE MEASUREMENT OF THE DAMPING IN ROLL OF STING-MOUNTED MODELS AND SOME INITIAL RESULTS FOR DELTA AND UNSWEPT TAPERED WINGS[1]

By William M. Bland, Jr., and Carl A. Sandahl

SUMMARY

A free-flight test technique with which the damping in roll of sting-mounted wings and wing-fuselage combinations can be obtained over the high subsonic, transonic, and supersonic speed range with rocket-propelled test vehicles is described, and some results for delta and unswept tapered wings are presented. Results for all the configurations tested show that damping in roll was maintained throughout the Mach number range investigated (0.6 to 1.7) and that subsonic damping-in-roll results agreed with theoretical values within experimental accuracy. In the lower supersonic region these results differ from the values predicted by linearized-flow theory; however, the agreement improved with increasing Mach number. Increased section thickness decreased the damping in roll of the delta wings throughout the Mach number range investigated.

INTRODUCTION

The Langley Pilotless Aircraft Research Division is utilizing two experimental techniques employing rocket-propelled test vehicles for the determination of the damping-in-roll derivative at high subsonic, transonic, and supersonic speeds at relatively large Reynolds numbers. One technique which is used for determining the damping in roll of wing-fuselage combinations is described in reference 1. The other technique which is used for determining the damping in roll of wings alone and of wing-fuselage combinations is described herein. The Reynolds numbers obtained with the use of this technique, although somewhat lower than those obtained with the technique of reference 1, are still fairly high (1×10^6 to 3×10^6).

---

[1]Supersedes recently declassified NACA RM L50D24, 1950.

Also presented herein are some initial results obtained by the present technique for a series of configurations having wings of aspect ratio 4. The configurations investigated included a delta-wing—fuselage combination having a wing made from a flat plate with beveled leading and trailing edges, two delta wings having 45° of leading-edge sweep - one with a 4-percent-thick symmetrical double-wedge airfoil section and the other with a 9-percent-thick symmetrical double-wedge airfoil section, and an unswept tapered wing having 0.5 taper ratio with a 4.6-percent-thick symmetrical double-wedge airfoil section.

SYMBOLS

C_{l_p}	damping-in-roll derivative, $\frac{dC_l}{d\left(\frac{pb}{2V}\right)}$
C_l	rolling-moment coefficient, $\frac{L}{qSb}$
$\frac{pb}{2V}$	wing-tip helix angle, radians
L	rolling moment, ft-lb
q	dynamic pressure, lb/sq ft
S	wing area, sq ft
b	wing span, ft
p	rolling velocity, radians/sec
V	flight-path velocity, ft/sec
M	Mach number
R	Reynolds number based on wing mean aerodynamic chord
c	wing chord, ft
$\bar{c}$	wing mean aerodynamic chord, $\frac{2}{S}\int_0^{b/2} c^2 dy$, ft
y	lateral coordinate

t	thickness, ft
A	aspect ratio obtained by extending wing leading and trailing edges to model center line
Λ	leading-edge sweep angle, deg
λ	taper ratio

METHOD

The general arrangement of the test vehicle is illustrated in figures 1 and 2. The wing under investigation was attached to a torsion spring balance arranged to form a sting mount in the nose of the test vehicle. In flight the entire test vehicle was forced to roll by the stabilizing fins, each of which was set at an angle of incidence. A rocket motor accelerated the test vehicle to the maximum Mach number, after which the test vehicle decelerated through the test Mach number range. Time histories of the rolling moment generated by the test wing, the flight-path velocity, and the rolling velocity were obtained. These data, in conjunction with atmospheric data obtained by radiosonde measurements, permitted the evaluation of the damping-in-roll derivative C_{l_p} as a function of Mach number.

A sample flight path illustrating the useful range of a flight and some typical conditions is shown in figure 3. Typical time histories of some of the measured quantities are shown in figure 4.

A photograph of a test vehicle mounted on the zero-length launcher is shown in figure 5.

INSTRUMENTATION

The torsion spring balance shown in figure 6 consisted of a shaft which transmitted the rolling moment generated by the test wing to a helical torsion spring which permitted angular movement relative to the test vehicle proportional to the rolling moment. The angular movements of the shaft were transmitted to a condenser-type pickup which was used in conjunction with standard NACA telemetry.

The rolling velocity was obtained by the method of reference 2 except that the telemeter and telemeter antenna performed the functions of the spinsonde described in the reference. The telemeter antenna

consisted of two rods which were inserted in the trailing edges of two diametrically opposed driving fins as shown in figure 1. This antenna arrangement produced the plane polarized radio signal required for the method of reference 2. The ground recording equipment was the same as that described in reference 2.

The flight-path velocity was measured by a Doppler radar velocimeter. The altitude, which was obtained by integrating the velocity-time curve, was correlated with radiosonde measurements of atmospheric conditions along the flight path made at the time of each test flight.

TEST CONFIGURATIONS

The configurations tested, all of which had an aspect ratio of 4.00, were (1) a delta-wing—fuselage combination employing an airfoil section having flat sides and symmetrically beveled leading and trailing edges (fig. 7), (2) a delta wing having 45° of leading-edge sweep with a 4-percent-thick symmetrical double-wedge airfoil section, (3) a delta wing having 45° of leading-edge sweep with a 9-percent-thick symmetrical double-wedge airfoil section, and (4) a wing having a taper ratio of 0.5 with an unswept 50-percent-chord line and a 4.6-percent-thick symmetrical double-wedge airfoil section. The geometric characteristics of the configurations tested are summarized in table I. Photographs of the test configurations are shown in figure 8. The wing surfaces were carefully ground and polished after being machined from steel plate. The distance from the trailing edge of the root chord of the wings to the nose of the test vehicle was held constant as shown in figure 1.

ACCURACY

The maximum possible systematic errors in the values of C_{l_p} presented herein due to the limitations of the measuring and recording systems are estimated to be within the following limits:

Delta wings		Unswept tapered wing	
M	Error in C_{l_p}	M	Error in C_{l_p}
1.7	±0.008	1.7	±0.015
1.4	±.013	1.2	±.030
.9	±.033	1.0	±.041
.7	±.053	.7	±.100

The variation of these possible errors is due to errors of constant magnitude included in some of the measured values; therefore, wherever the measured rolling moment or rolling velocity, or both, decreases, the respective errors become a larger part of the measured values and increase the possible error.

An error in the determination of C_{l_p} may exist because of the necessity of neglecting the tare rolling moment; that is, the rolling moment which might exist at $\frac{pb}{2V} = 0$ because of inaccuracies in model construction. However, the results obtained for models with only nominal differences presented herein agree well within the aforementioned limits.

Any contributions to the possible error by the drag of the test configurations and temperature variations on the spring balance are negligible when compared with the errors previously tabulated.

The measured rolling moment included a moment equal to the product of the moment of inertia of the test assembly (wings and contributing parts of the torsion spring balance) and the instantaneous acceleration in roll. In the present investigation the inertia rolling moment produced a maximum error in C_{l_p} of -0.002; therefore, the data are presented without correction for this error.

RESULTS AND DISCUSSION

The results for all the wings investigated are presented in figure 9 as curves of rolling-moment coefficient C_l, wing-tip helix angle $\frac{pb}{2V}$, and damping-in-roll derivative C_{l_p} as functions of Mach number. The results presented in figures 9(b) and 9(c) for models with nominal differences indicate the repeatability of the experimental results. The two models of configuration 3 were identical, except for the incidence of the driving tail fins. The two different tail-incidence values employed resulted in the two levels of $\frac{pb}{2V}$ obtained for this configuration. The variation of Reynolds number with Mach number for the configurations investigated is shown in figure 10.

Delta Wings

In figure 11(a) the variation of C_{l_p} with Mach number for all the delta wings is summarized and compared with theoretical values in

the subsonic and supersonic speed ranges. The results show that damping in roll is maintained for each configuration throughout the Mach number range investigated (0.6 to 1.7). For the delta wings without fuselages, increasing the wing thickness ratio from 0.040 to 0.090 reduced the damping in roll throughout the speed range included in these tests, particularly in the region approaching Mach number 1.0. At the higher supersonic Mach numbers the thickness effect decreased. At the lower supersonic Mach numbers the wing-fuselage combination had greater damping in roll than the wing-alone configurations. This increase in C_{l_p} may be due to a fuselage effect, as indicated in reference 3, for low body-diameter—wing-span ratios under conditions where the wing leading edge is highly swept when compared with the Mach cone. In the low supersonic range the experimental results obtained for each of these wings are considerably lower than those calculated by the linearized-flow methods for wings of zero thickness (ref. 4); however, the agreement improves with increasing Mach number and decreasing thickness ratio. In the subsonic speed range the results agree within experimental accuracy with values from reference 5 to which approximate corrections for the effects of compressibility have been applied by utilizing the Glauert-Prandtl transformation as described in reference 6.

Unswept Tapered Wing

Figure 11(b) compares the variation of C_{l_p} with Mach number obtained for the unswept tapered wing with theoretical results and shows that damping in roll is maintained throughout the Mach number range investigated. At subsonic speeds the agreement with calculated damping-in-roll values to which compressibility corrections have been applied (ref. 7) is within experimental accuracy. In the supersonic range the agreement with theoretical values based on linearized-flow equations (ref. 4) improves with increasing Mach number.

An indication of the effect of wing plan form can be obtained from figure 11 by comparing the results for the 4-percent-thick delta wings with those for the unswept tapered wing. Except at the lowest Mach numbers investigated the damping in roll of the tapered wing is considerably larger than that of the delta wings.

CONCLUSIONS

Measurements by means of a technique utilizing rocket-propelled test vehicles of the damping in roll of several sting-mounted delta wings and a sting-mounted unswept tapered wing indicate the following conclusions:

1. For all wings tested, the damping in roll was maintained throughout the Mach number range investigated (0.6 to 1.7). Increasing the thickness ratio of the delta wings from 0.040 to 0.090, however, decreased the damping in roll throughout the Mach number range investigated, particularly at Mach numbers slightly less than 1.0.

2. At the lower subsonic speeds investigated the agreement between theory and experiment was within experimental accuracy. At low supersonic speeds poor agreement was obtained between the experimental values and those predicted by the linearized theory; the agreement improved with increasing Mach number. Decreasing the thickness ratio of the delta wings improved the agreement with the linearized theory.

Langley Aeronautical Laboratory,
National Advisory Committee for Aeronautics,
Langley Field, Va., May 2, 1950.

REFERENCES

1. Edmondson, James L., and Sanders, E. Claude, Jr.: A Free-Flight Technique for Measuring Damping in Roll by Use of Rocket-Powered Models and Some Initial Results for Rectangular Wings. NACA RM L9I01, 1949.

2. Harris, Orville R.: Determination of the Rate of Roll of Pilotless Aircraft Research Models by Means of Polarized Radio Waves. NACA TN 2023, 1950.

3. Lomax, Harvard, and Heaslet, Max. A.: Damping-in-Roll Calculations for Slender Swept-Back Wings and Slender Wing-Body Combinations. NACA TN 1950, 1949.

4. Piland, Robert O.: Summary of the Theoretical Lift, Damping-in-Roll, and Center-of-Pressure Characteristics of Various Wing Plan Forms at Supersonic Speeds. NACA TN 1977, 1949.

5. Goodman, Alex, and Adair, Glenn H.: Estimation of the Damping in Roll of Wings Through the Normal Flight Range of Lift Coefficient. NACA TN 1924, 1949.

6. Polhamus, Edward C.: A Simple Method of Estimating the Subsonic Lift and Damping in Roll of Sweptback Wings. NACA TN 1862, 1949.

7. Fisher, Lewis R.: Approximate Corrections for the Effects of Compressibility on the Subsonic Stability Derivatives of Swept Wings. NACA TN 1854, 1949.

TABLE I

GEOMETRIC CHARACTERISTICS OF CONFIGURATIONS TESTED

Configuration	Model	Wing plan form	Body	Wing thickness ratio	Airfoil section	Wing area, S (sq ft)	Aspect ratio, A	Wing span, b (ft)	Mean aerodynamic chord, $\bar{c}$ (ft)
1		Delta; $\Lambda = 45^\circ$	With	Variable	Beveled plate	0.188	4.00	0.867	0.288
2	a b	Delta; $\Lambda = 45^\circ$	Without	0.040	Symmetrical double wedge	.188	4.00	.867	.288
3	a b	Delta; $\Lambda = 45^\circ$	Without	.090	Symmetrical double wedge	.188	4.00	.867	.288
4		c/2 line unswept; taper ratio, 0.5	Without	.046	Symmetrical double wedge	.188	4.00	.867	.225

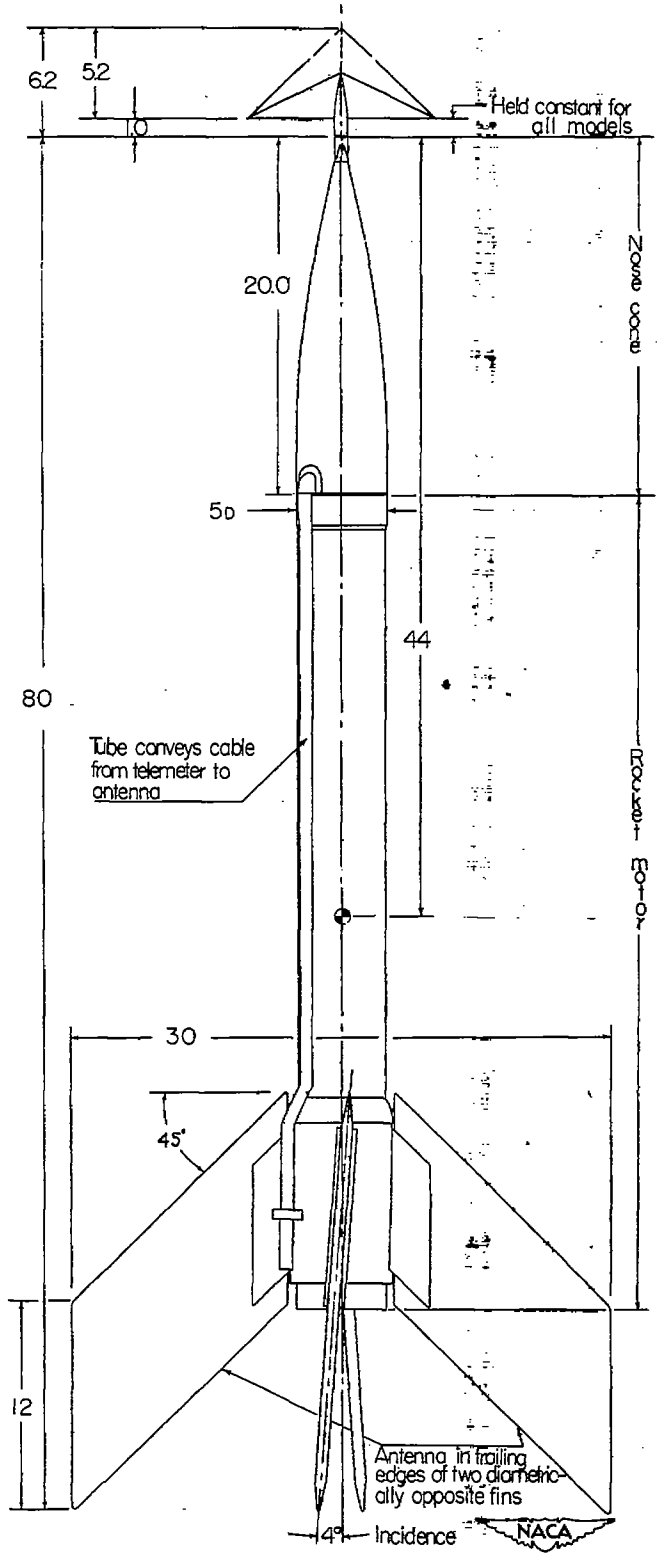

Figure 1.- General arrangement of a model with all dimensions in inches.

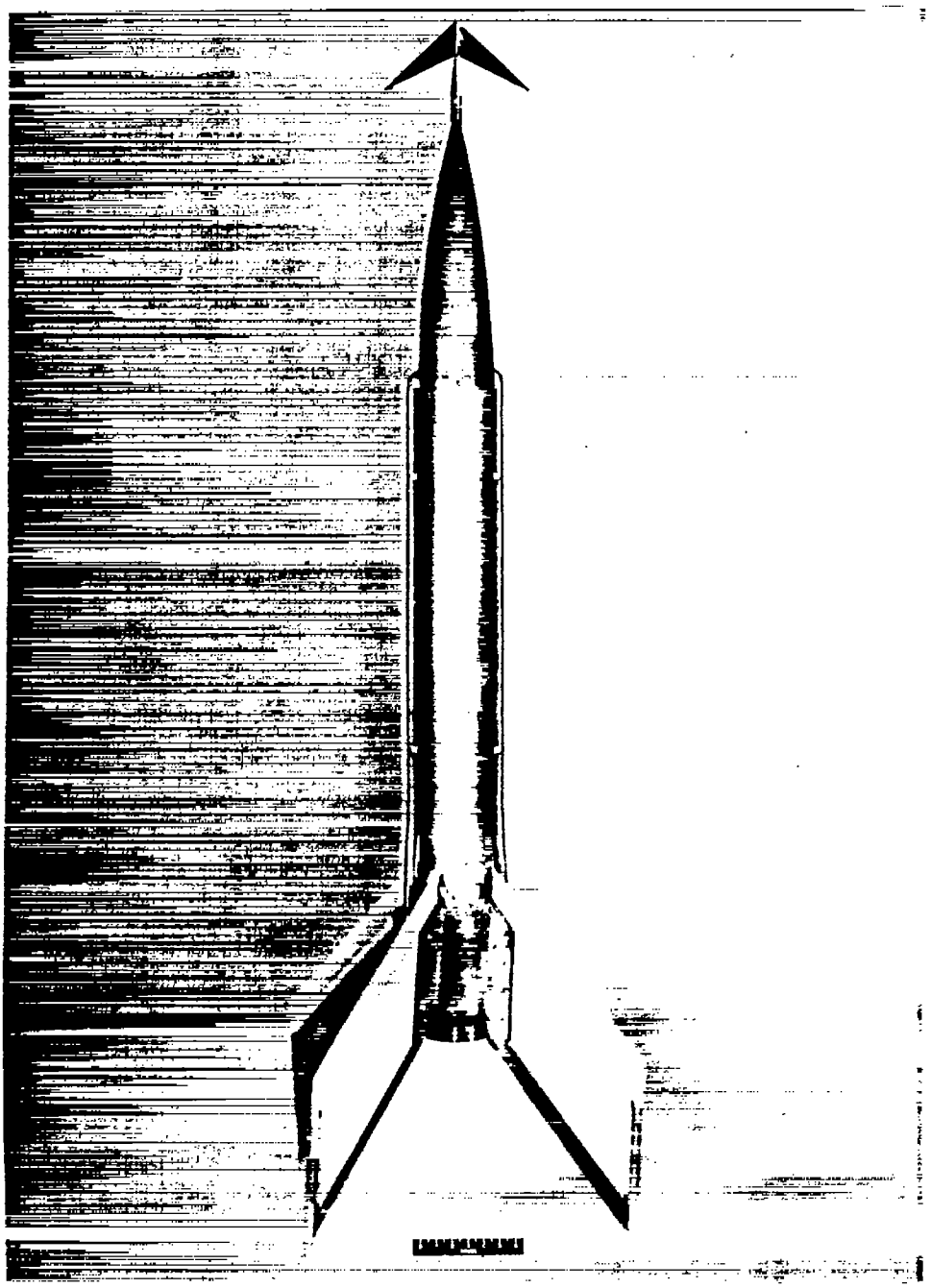

NACA
L-61603.2

Figure 2.- Typical test vehicle with test wing attached.

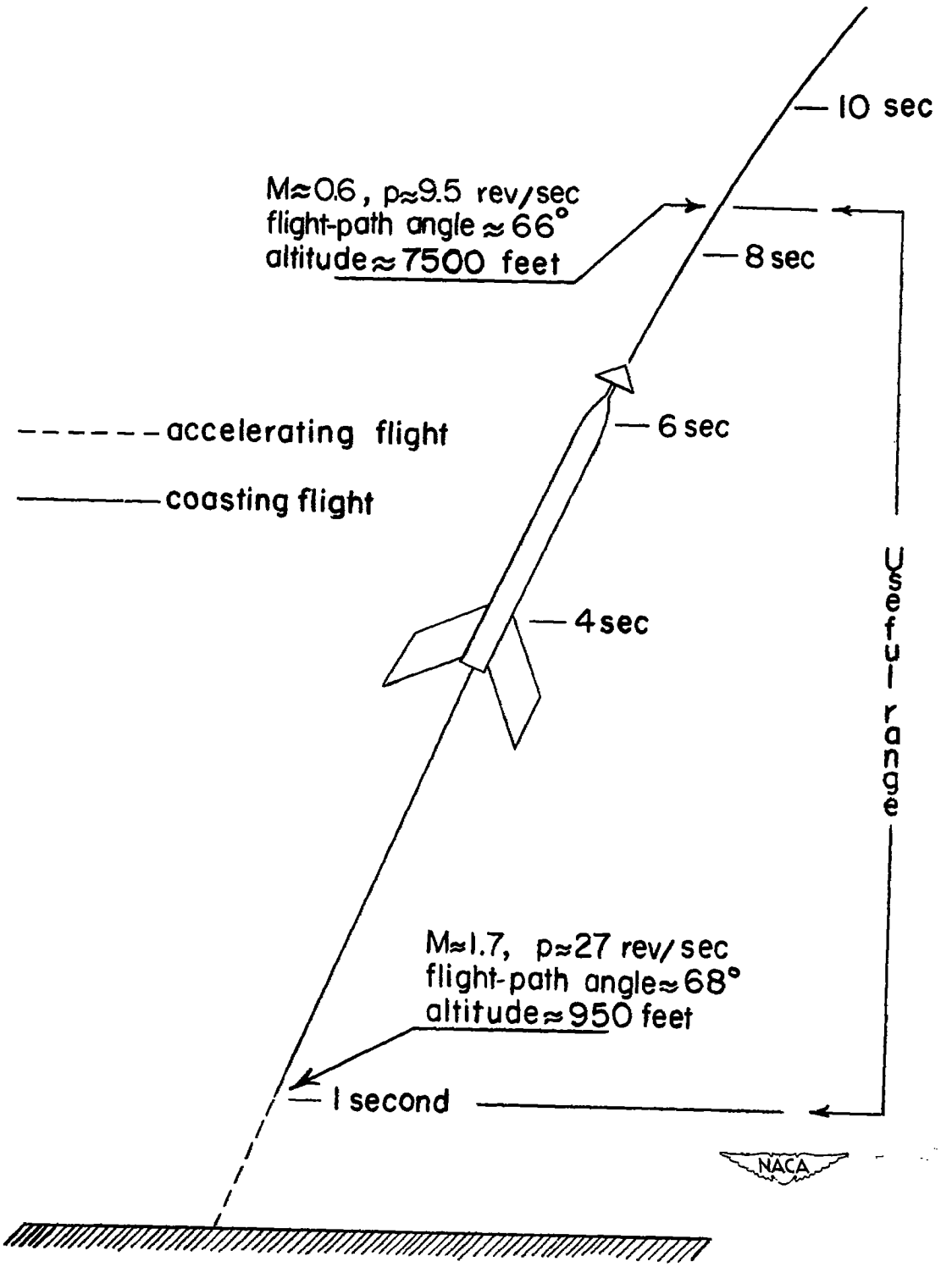

Figure 3.- Sample flight path with performance figures.

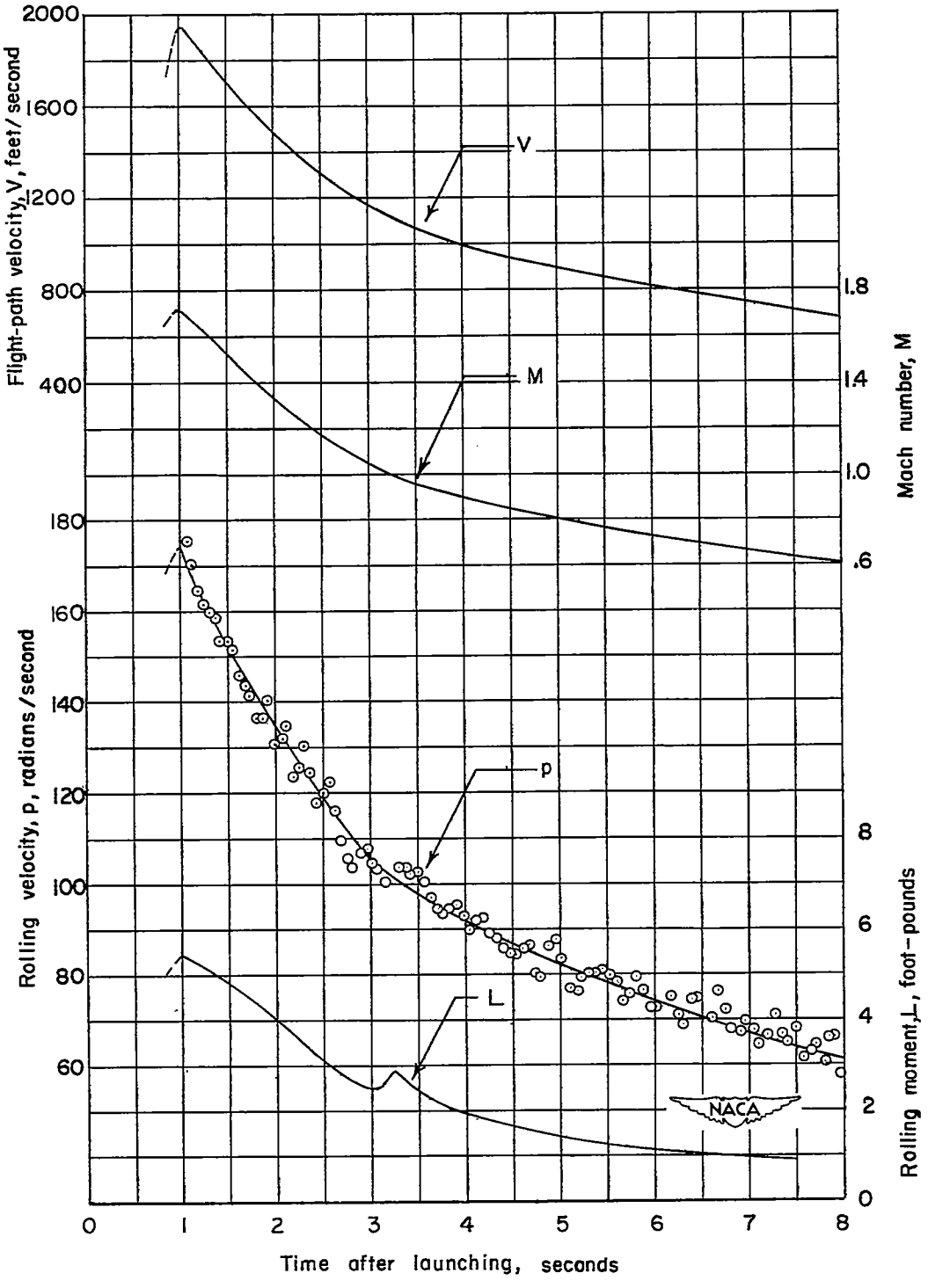

Figure 4.- Variation with time of flight-path velocity, Mach number, rolling velocity, and rolling moment for configuration 2(b).

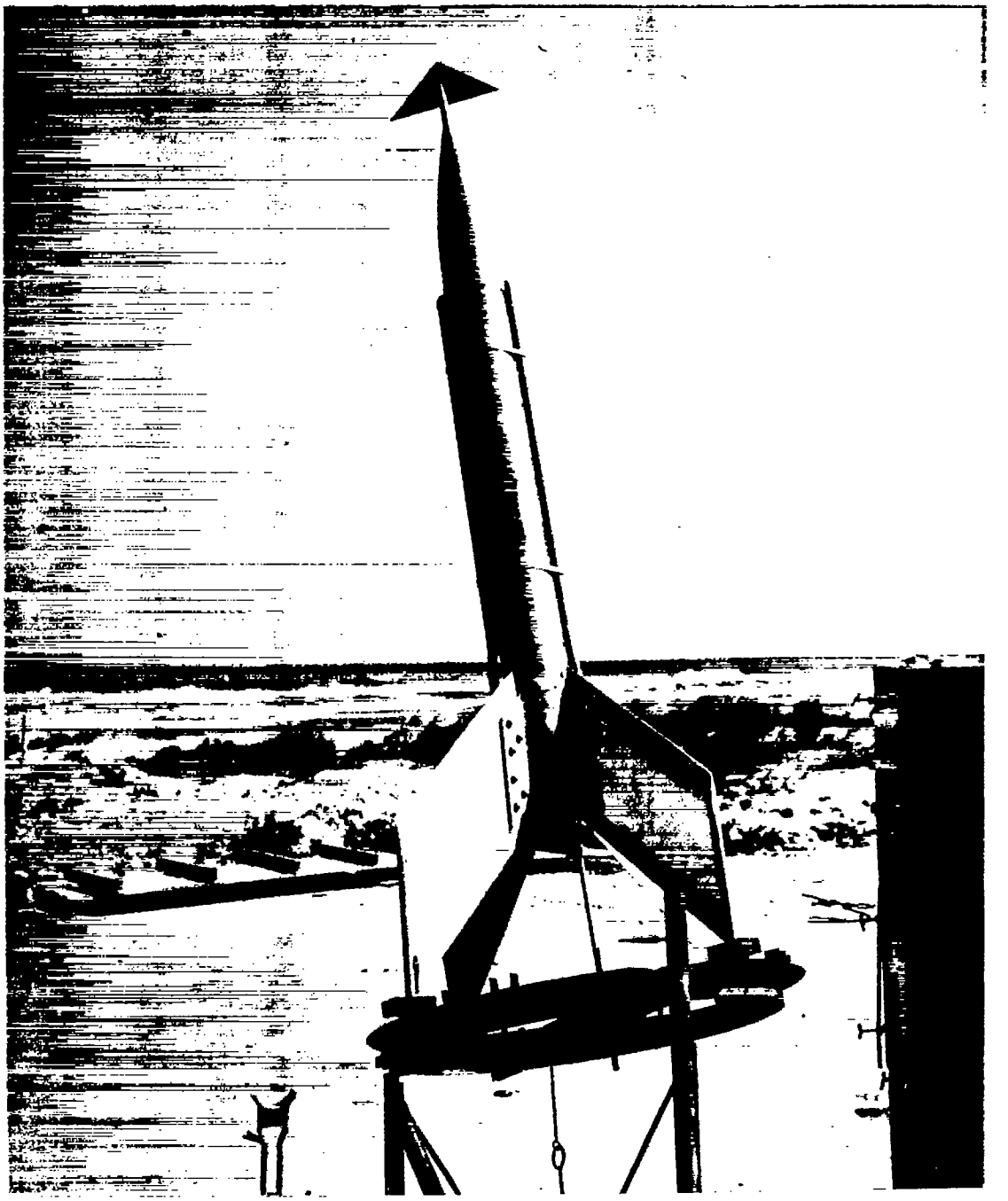

Figure 5.- Test vehicle on zero-length launcher.

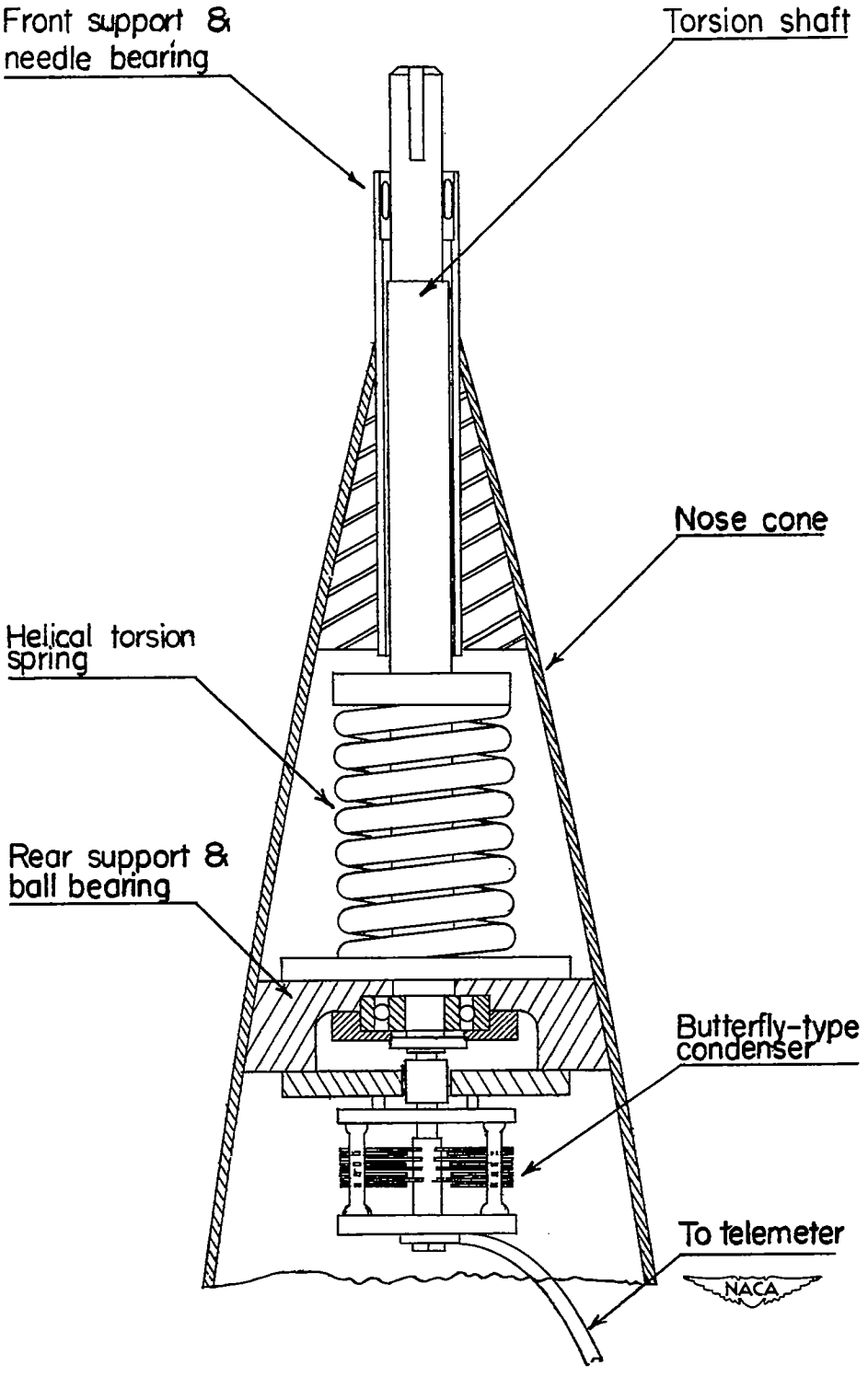

Figure 6.- Nose cone interior showing spring balance and capacitance pickup.

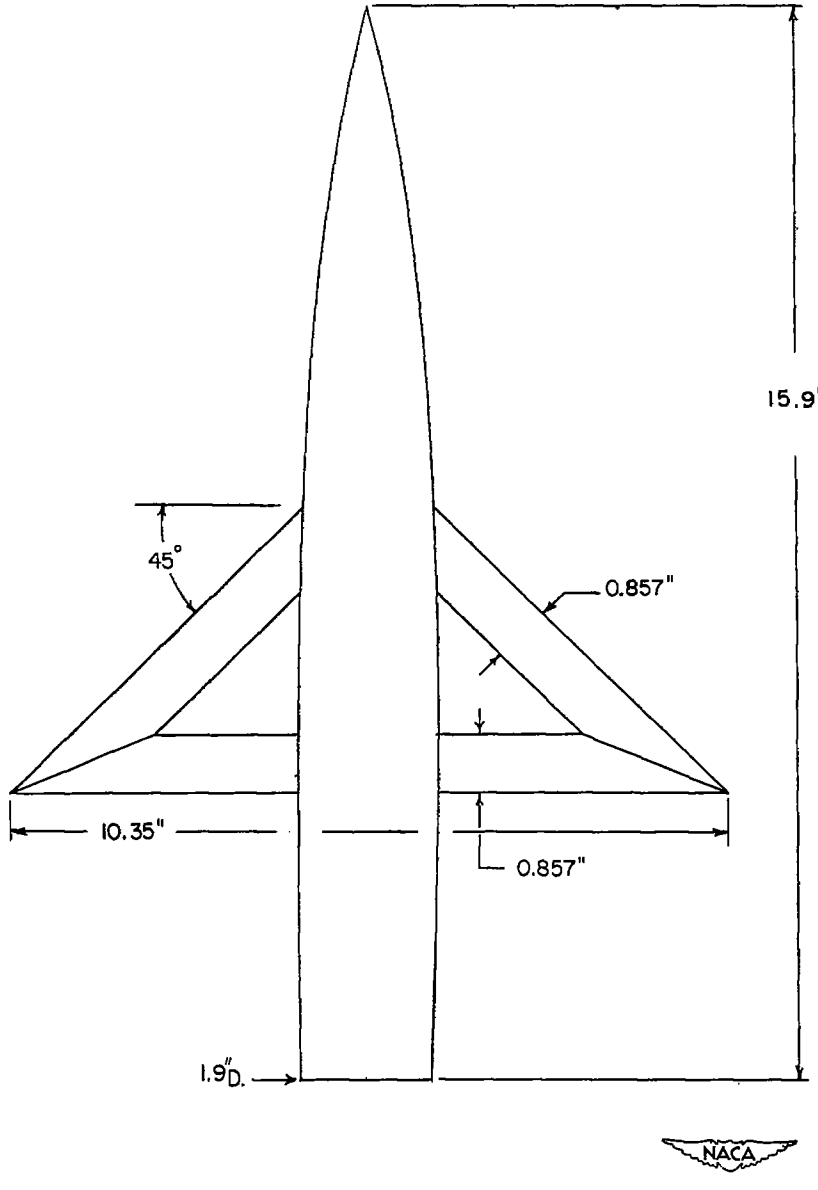

Figure 7.- Configuration 1. Fuselage has a circular cross section through which the wing passes diametrically. Wing was made of 0.146 steel plate with beveled leading and trailing edges.

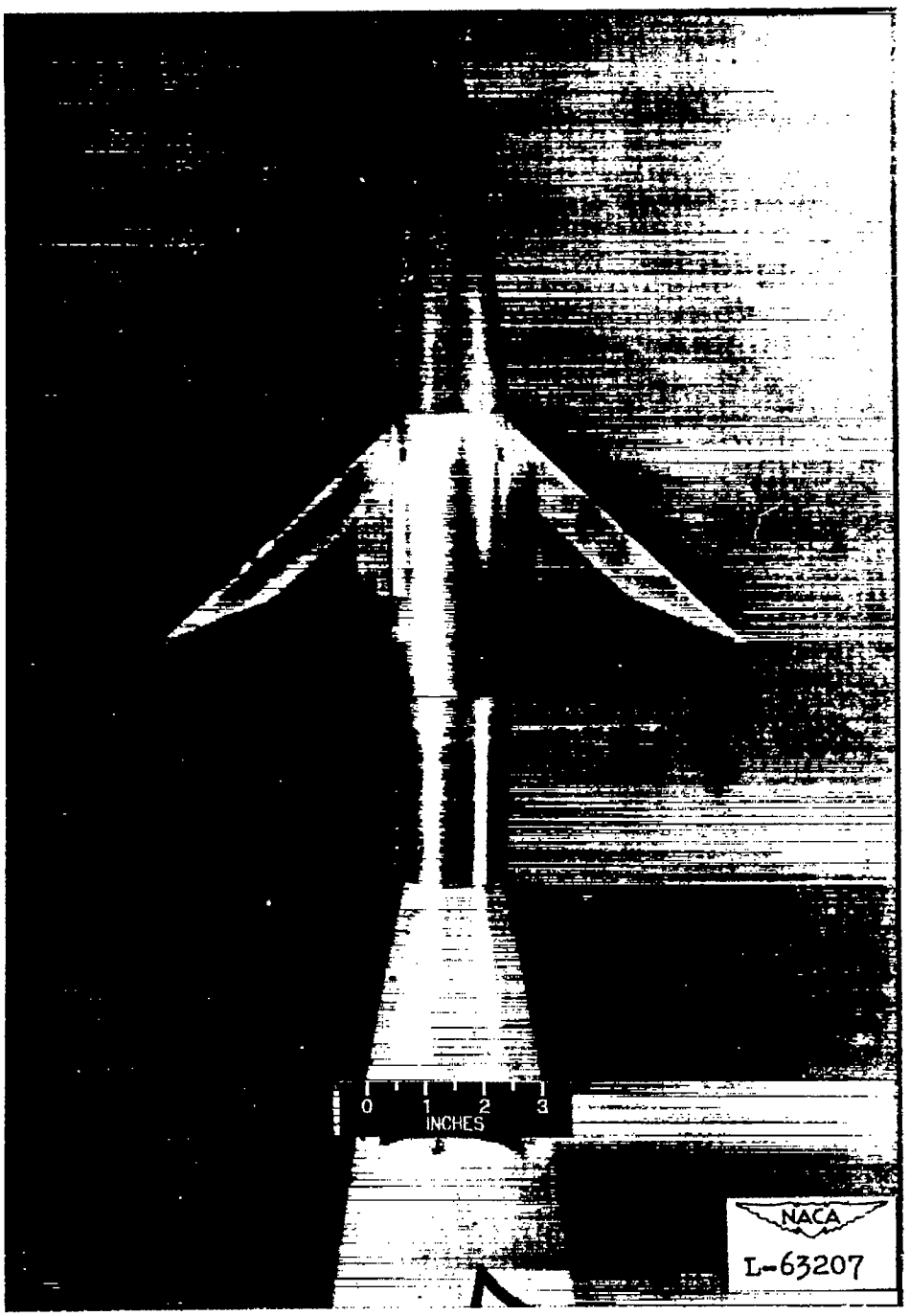

(a) Configuration 1.

Figure 8.- Configurations tested.

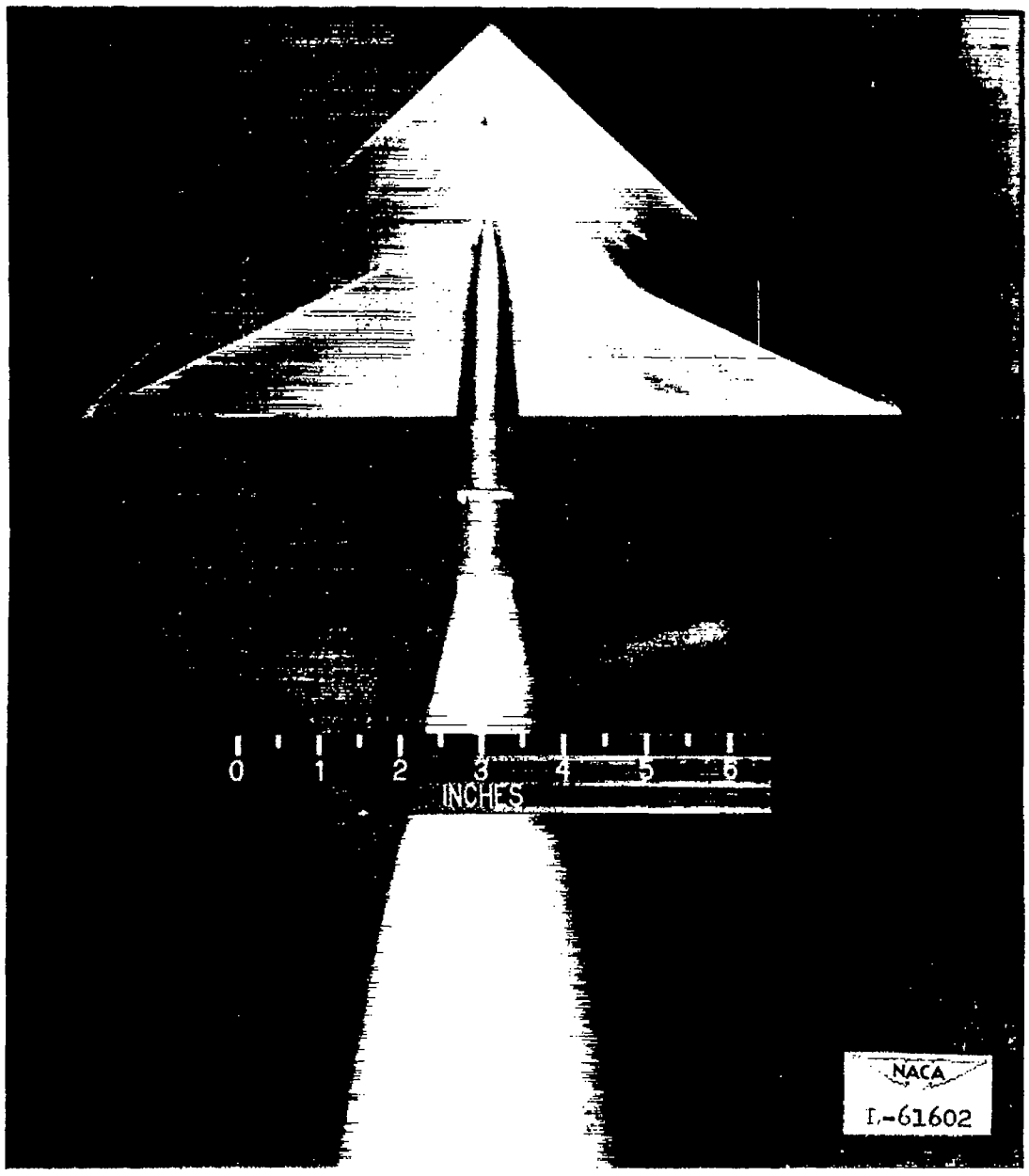

(b) Configurations 2 and 3.

Figure 8.- Continued.

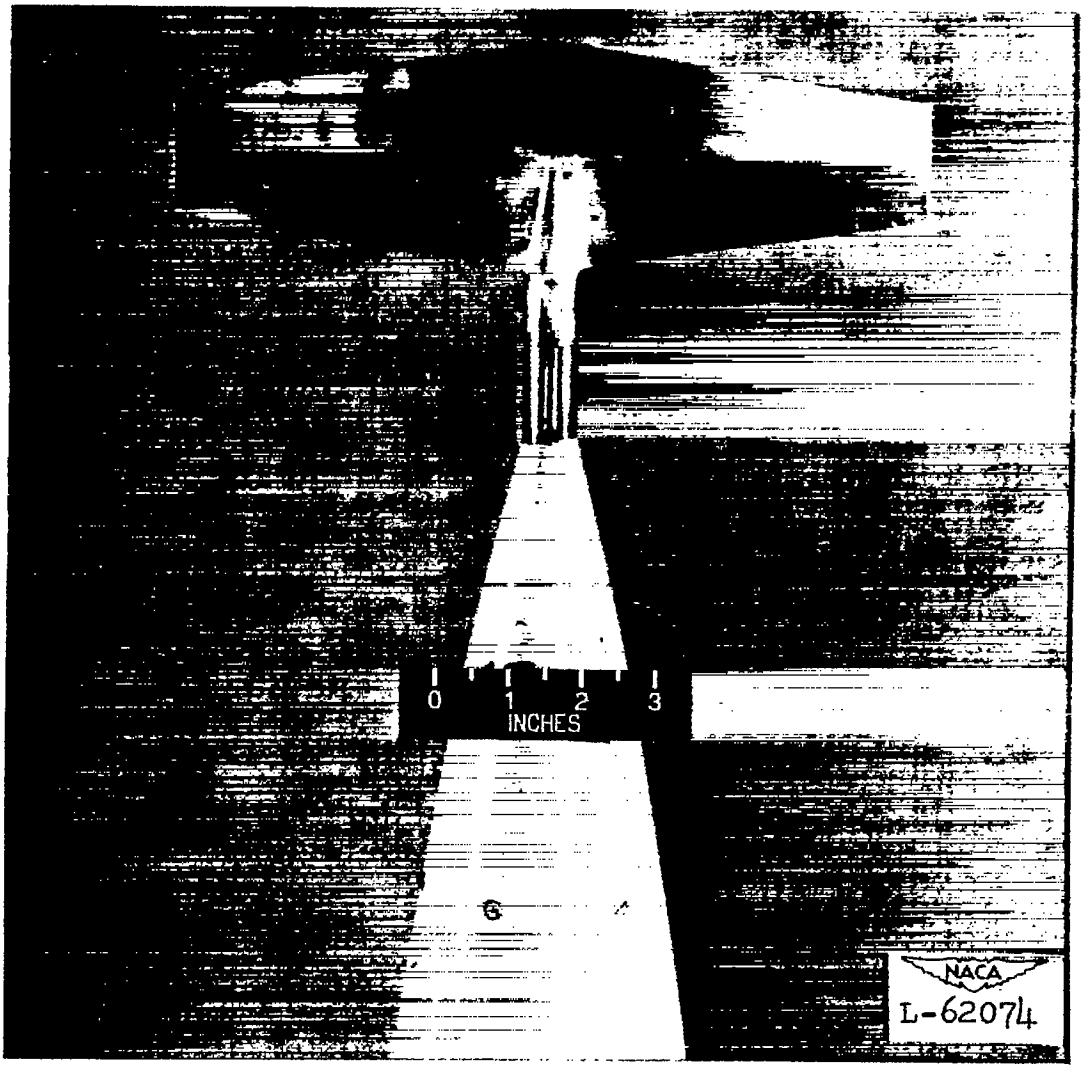

(c) Configuration 4.

Figure 8.- Concluded.

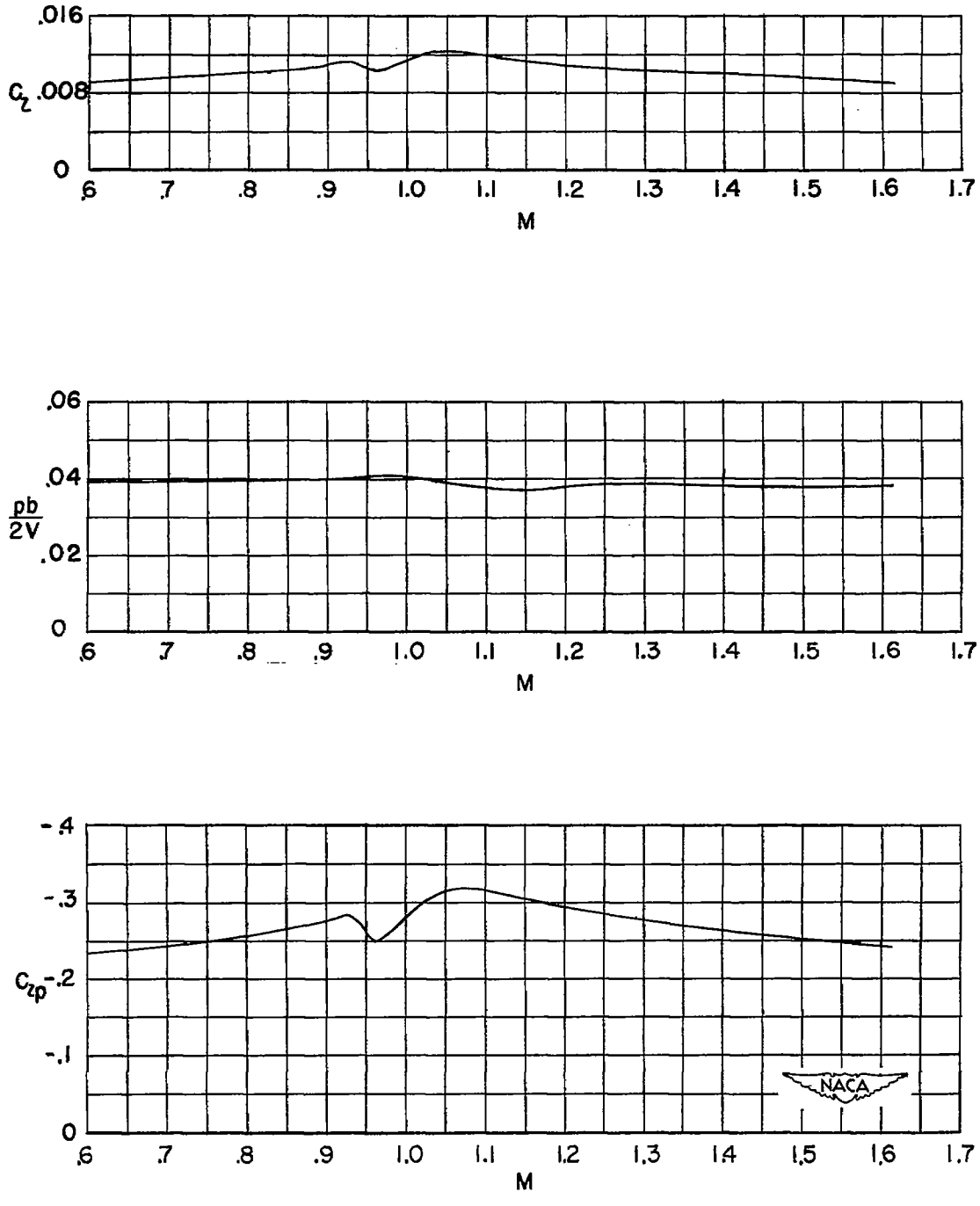

(a) Configuration 1, 45° delta-wing and fuselage combination.

Figure 9.- Experimental results.

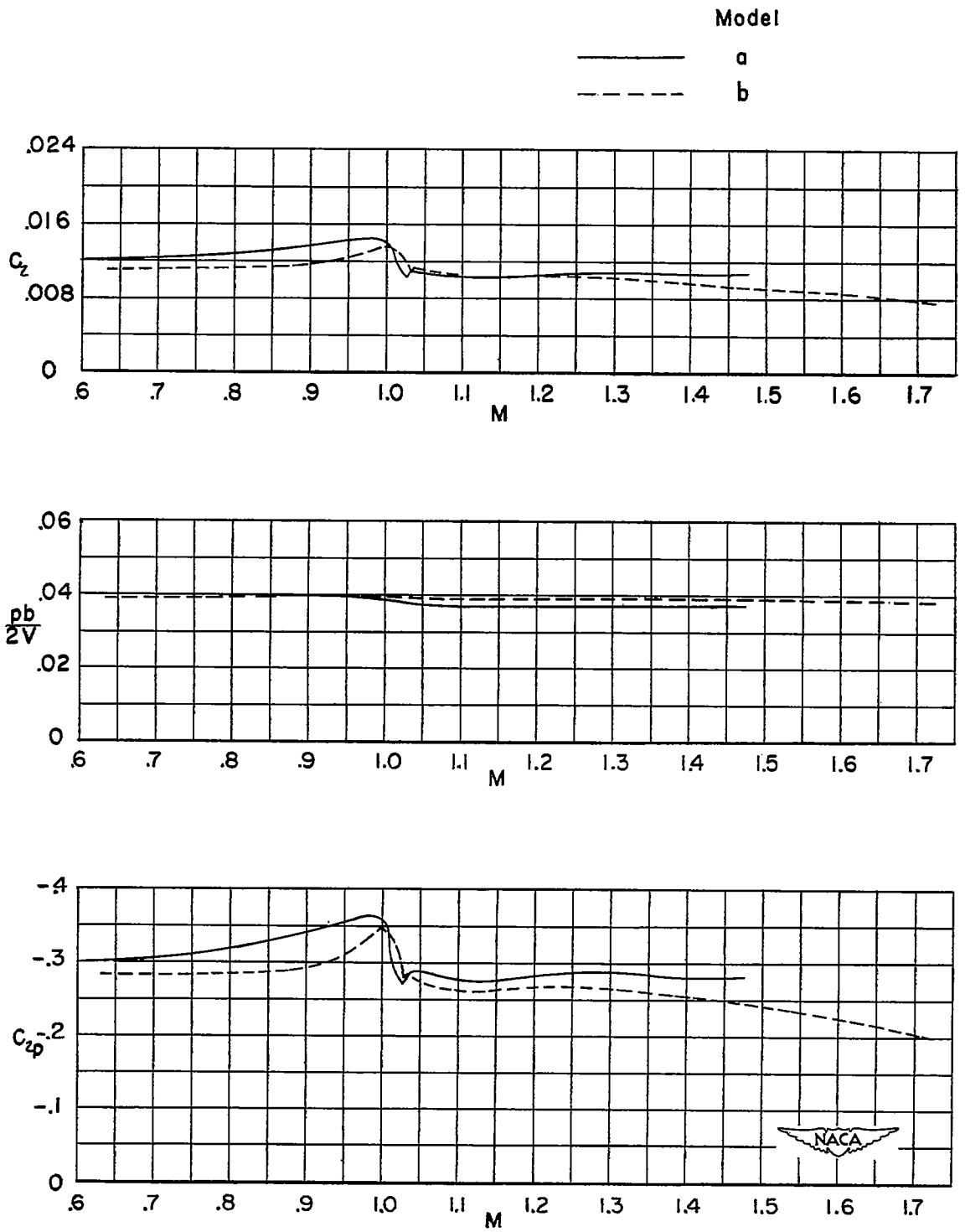

(b) Configuration 2, delta wing, $\Lambda = 45^\circ$, $t/c = 0.040$.

Figure 9.- Continued.

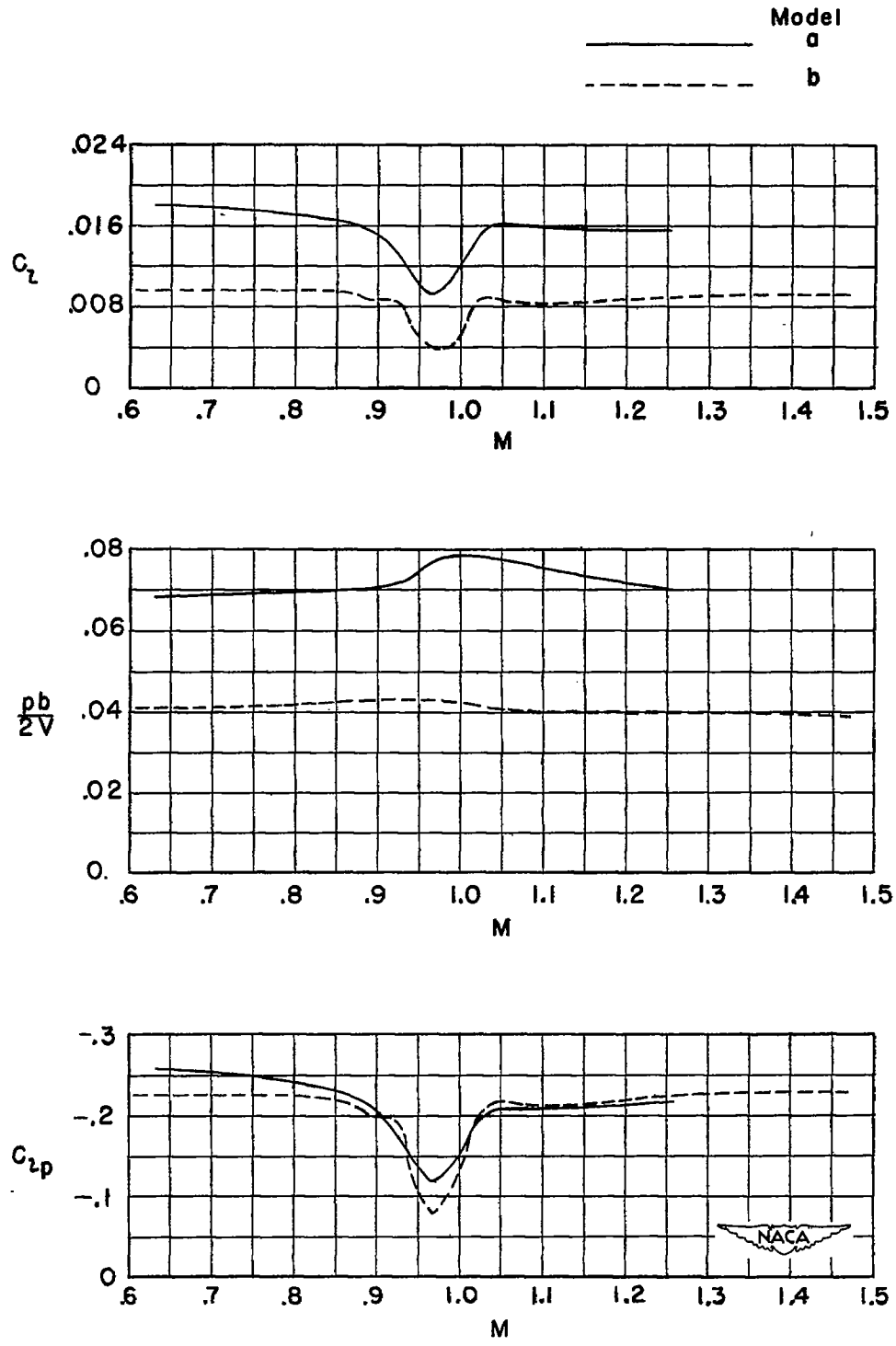

(c) Configuration 3, delta wing, $\Lambda = 45^\circ$, $t/c = 0.090$.

Figure 9.- Continued.

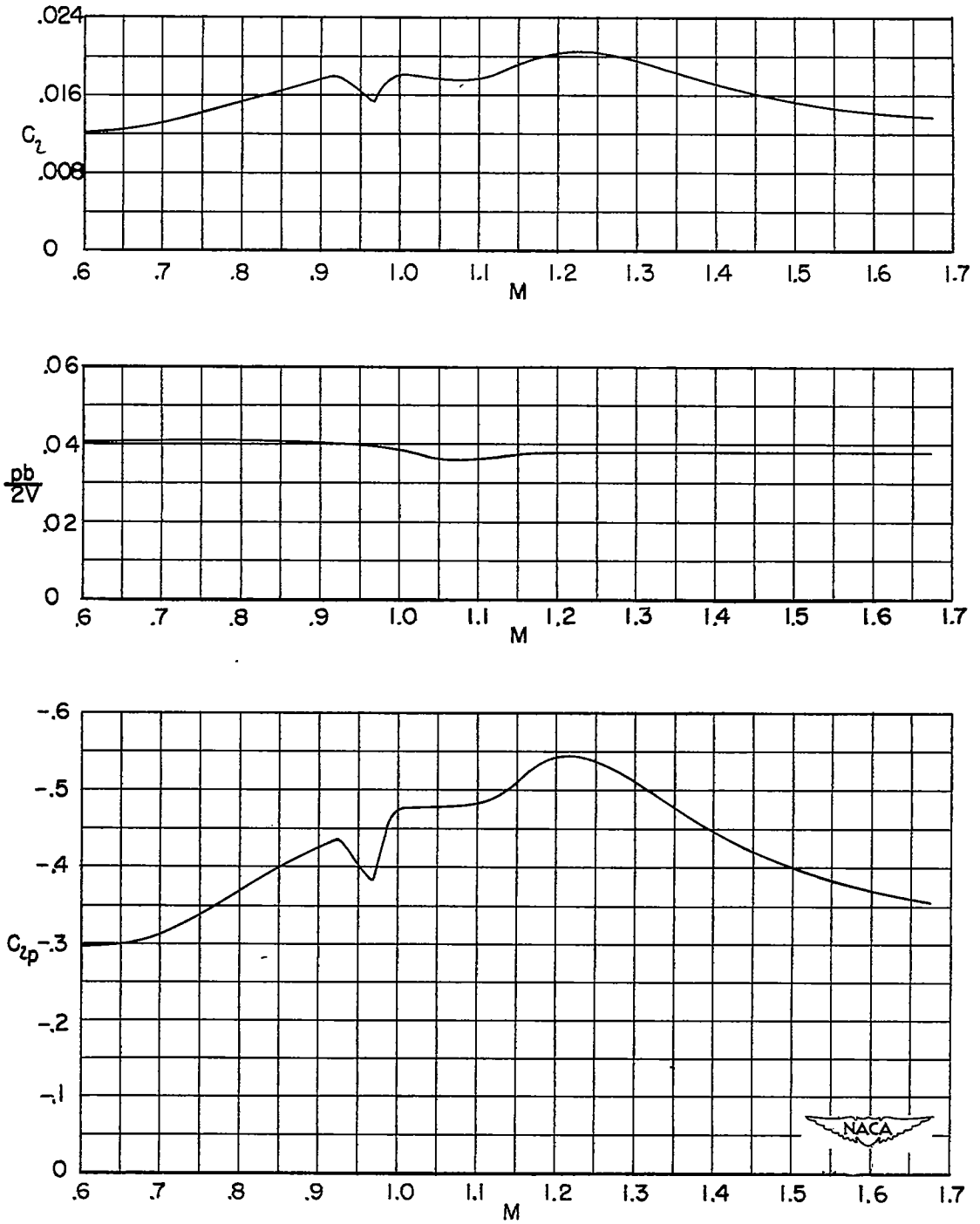

(d) Configuration 4, unswept tapered wing, $\lambda = 0.5$, $t/c = 0.046$.

Figure 9.- Concluded.

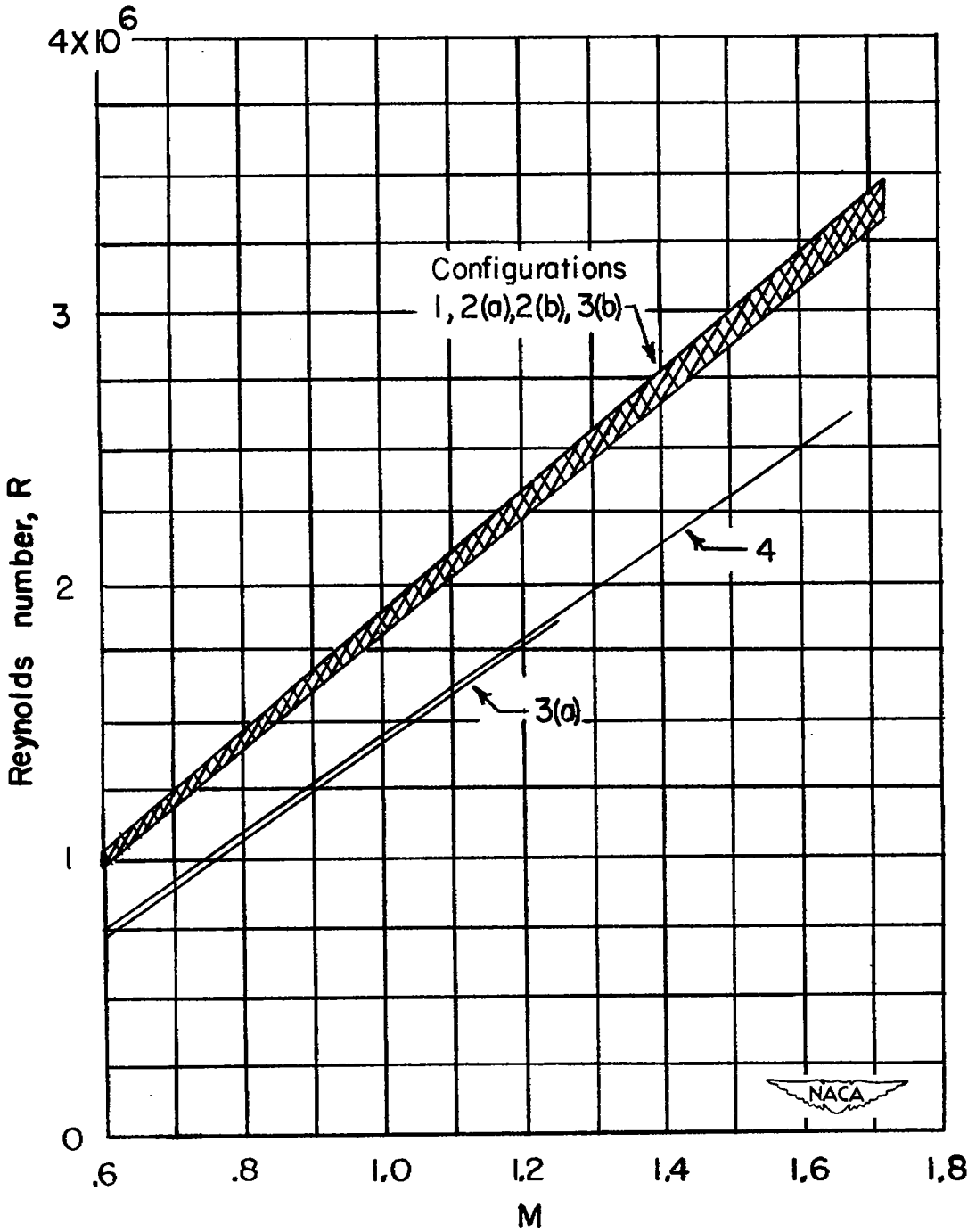

Figure 10.- Variation of Reynolds number with Mach number for the range of climatic conditions encountered during the tests.

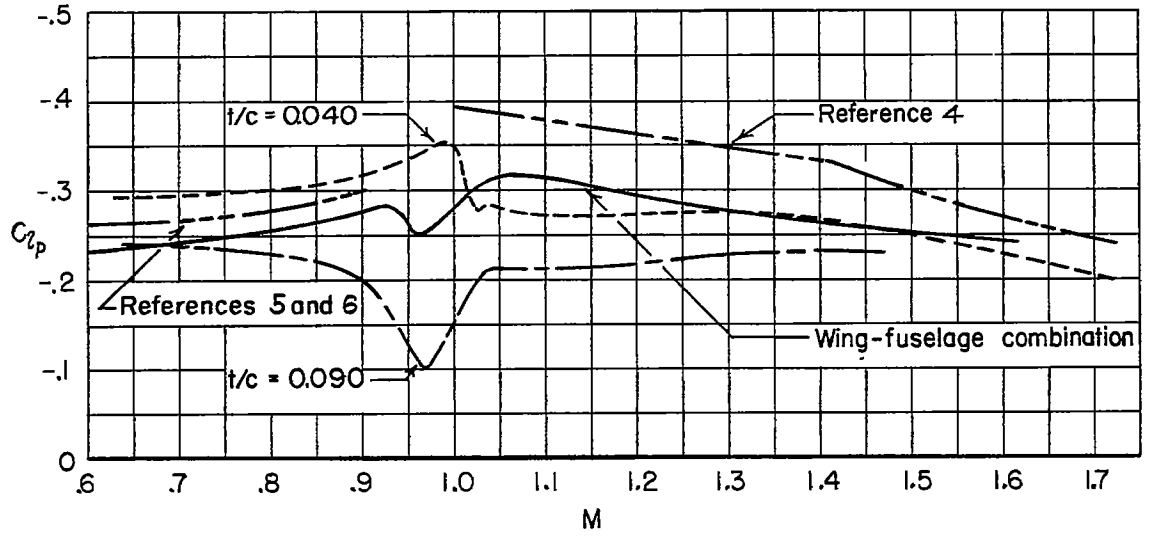

(a) Delta wings.

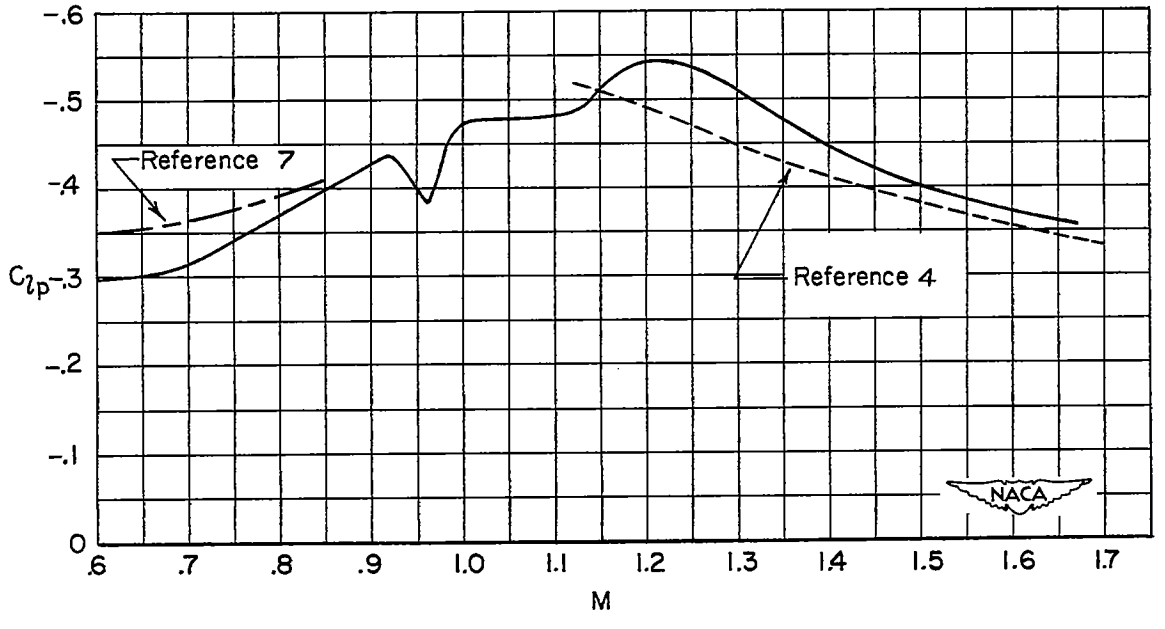

(b) Unswept tapered wing.

Figure 11.- Experimental results compared with theoretical results.

NACA-Langley - 5-17-55 - 1000